

# Amyloids



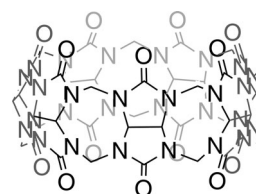
## Supramolecular Inhibition of Amyloid Fibrillation by Cucurbit[7]uril\*\*

Hong Hee Lee, Tae Su Choi, Shin Jung C. Lee, Jong Wha Lee, Junghong Park, Young Ho Ko, Won Jong Kim, Kimoon Kim,\* and Hugh I. Kim\*

**Abstract:** Amyloid fibrils are insoluble protein aggregates comprised of highly ordered  $\beta$ -sheet structures and they are involved in the pathology of amyloidoses, such as Alzheimer's disease. A supramolecular strategy is presented for inhibiting amyloid fibrillation by using cucurbit[7]uril (CB[7]). CB[7] prevents the fibrillation of insulin and  $\beta$ -amyloid by capturing phenylalanine (Phe) residues, which are crucial to the hydrophobic interactions formed during amyloid fibrillation. These results suggest that the Phe-specific binding of CB[7] can modulate the intermolecular interaction of amyloid proteins and prevent the transition from monomeric to multimeric states. CB[7] thus has potential for the development of a therapeutic strategy for amyloidosis.

Amyloid fibrils are self-assembled insoluble protein aggregates comprised of highly ordered  $\beta$ -sheet structures. These fibrils are related to amyloidoses, such as Alzheimer's disease,<sup>[1]</sup> Parkinson's disease,<sup>[2]</sup> and spongiform encephalopathy.<sup>[3]</sup> The complicated fibrillation processes in amyloidoses involve a large number of structural species and highly diverging mechanisms, which make these processes extremely difficult to control.<sup>[4]</sup> Developing methods for inhibiting the formation of these self-assembled fibrils is still challenging despite its therapeutic significance.<sup>[5]</sup> Small-molecule inhibitors have been widely investigated for amyloid inhibition.<sup>[5,6]</sup>

For example,  $\beta$ -cyclodextrins<sup>[6b]</sup> and molecular tweezers<sup>[6c]</sup> targeted to Tyr and Lys, respectively, are known to inhibit amyloid fibrillation. However, the binding affinity of these molecules for their target moieties are generally low ( $K_a \approx 10^2$ – $10^4$  M<sup>-1</sup>), and their applicability and detailed mechanisms are still poorly defined. Therefore, a "rational" design with mechanistic detail is necessary for a breakthrough in developing a new molecular method for the inhibition of amyloid formation. Phenylalanine (Phe) residues are known to initiate and enhance the hydrophobic clustering of amyloid proteins,<sup>[7]</sup> which is the driving force in amyloidosis.<sup>[8]</sup> Since cucurbit[7]uril (CB[7]; Scheme 1), a member of the synthetic



**Scheme 1.** The structure of cucurbit[7]uril (CB[7]).

receptor family cucurbit[*n*]uril ( $n = 5$ – $8$ ,  $10$ ,  $14$ ),<sup>[9]</sup> is known to bind specifically and tightly ( $K_a \approx 10^4$ – $10^7$  M<sup>-1</sup>) to Phe residues in proteins,<sup>[10]</sup> blocking the hydrophobic interactions of the residues by encapsulating them with CB[7] could be an effective approach for the inhibition of amyloid formation. Herein, we report an innovative supramolecular strategy to inhibit amyloid processes by capturing the Phe residues of amyloid proteins with CB[7]. We chose insulin (Ins) and  $\beta$ -amyloid peptides (A $\beta$ 40 and A $\beta$ 42) as representative structured and unstructured amyloid proteins, respectively. The results show that CB[7] effectively inhibits the self-assembly process of amyloidogenic proteins by increasing the kinetic barrier of fibrillation with a thermodynamic advantage.<sup>[11]</sup>

We first investigated the effect of CB[7] on Ins ( $10 \mu\text{M}$ ; Figure 1a) fibrillation over a series of Ins:CB[7] ratios by using a thioflavin T (ThT) spectroscopic assay to monitor the kinetics of  $\beta$ -sheet formation (Figure 1b). Ins fibrillation was conducted in 20 mM sodium phosphate buffer (SPB, pH 7.4) at 50 °C. An *ex situ* ThT assay was used to prevent ThT from influencing the fibrillation kinetics.<sup>[12]</sup> CB[7] successfully inhibited fibrillation at Ins:CB[7] ratios of 1:0.5 or with a higher ratio of CB[7] to Ins as suggested by the fact that there was little or no change in the ThT fluorescence intensity. No trace of amyloid fibrils was observed in the TEM images of Ins with CB[7] after a 42 h incubation, except at a ratio of 1:0.5 (Figure 1c). The short, low-abundance aggregates observed at an Ins/CB[7] ratio of 1:0.5 implies that less than equimolar concentrations of CB[7] can inhibit the formation of elongated fibrils. On the basis of ThT assay, further fibril

[\*] H. H. Lee,<sup>[†]</sup> T. S. Choi,<sup>[†]</sup> S. J. C. Lee, J. W. Lee, J. Park, Prof. Dr. W. J. Kim, Prof. Dr. K. Kim, Prof. Dr. H. I. Kim  
Department of Chemistry  
Pohang University of Science and Technology  
Pohang, 790-784 (Republic of Korea)  
E-mail: hughkim@postech.edu

J. Park, Dr. Y. H. Ko, Prof. Dr. W. J. Kim, Prof. Dr. K. Kim  
Center for Self-assembly and Complexity  
Institute for Basic Science  
Pohang University of Science and Technology  
Pohang, 790-784 (Republic of Korea)  
E-mail: kkim@postech.ac.kr

Prof. Dr. K. Kim, Prof. Dr. H. I. Kim  
Division of Advanced Materials Science  
Pohang University of Science and Technology  
Pohang, 790-784 (Republic of Korea)

[†] These authors contributed equally to this work.

[\*\*] This work was supported by Basic Science Research (2013R1A1A2008974) through the National Research Foundation (NRF) of Korea funded by the Ministry of Science, ICT and Future Planning (MSIP), and by the Institute for Basic Science (IBS) [CA1403]. T.S.C. and S.J.C.L. acknowledge support from a T J Park Fellowship and NRF Grant (NRF-2011-Global Ph.D. Fellowship program), respectively.

Supporting information (including experimental details) for this article is available on the WWW under <http://dx.doi.org/10.1002/anie.201402496>.

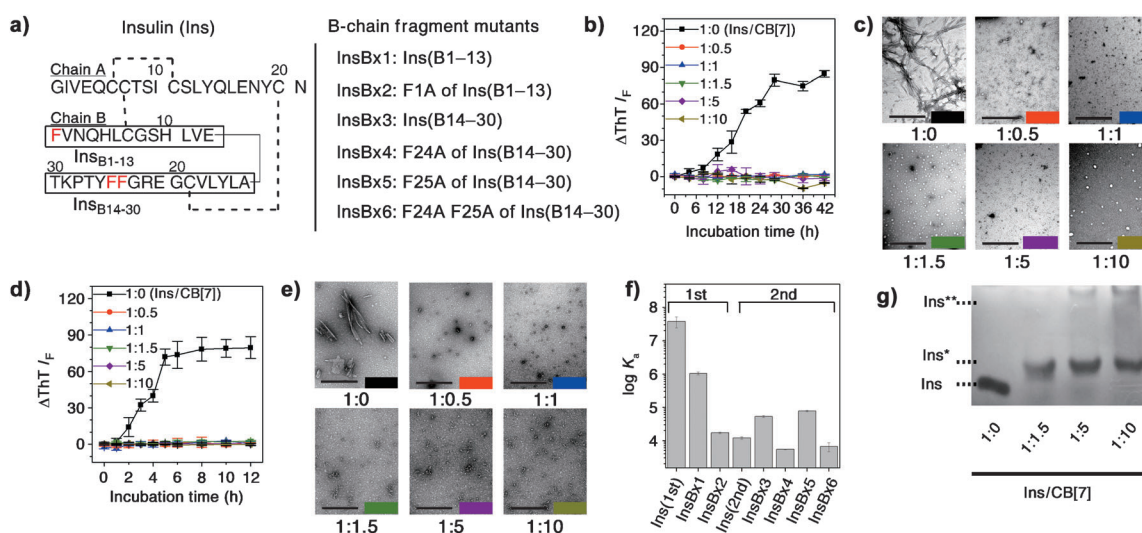


**Figure 1.** a) The sequence of insulin (Ins) and its B-chain fragment mutants. Mutation sites are marked in red. b) Fibrillation kinetics of Ins with a series of Ins:CB[7] ratios in 20 mM SPB pH 7.4. c) TEM images of Ins fibril by Ins:CB[7] ratio after 42 h. d) Fibrillation kinetics of Ins with a series of Ins:CB[7] ratios at pH 2.7 [0.1% formic acid (v/v)]. e) TEM images of Ins fibrils by Ins:CB[7] ratio after 12 h. f) Bar plots for the equilibrium association constant ( $K_a$ ) for Ins with CB[7] as measured by ITC (Figure S2). g) Native PAGE for the binding event that results in the formation of Ins-CB[7]. The Ins-1CB[7] complex (Ins\*) corresponds to a Phe-B1-CB[7] complex. The Ins-2CB[7] complex (Ins\*\*) indicates the secondary binding event Phe-B24-CB[7]. The concentration of Ins was 10  $\mu$ M. Scale bars: 500 nm.

growth was also inhibited when CB[7] (100  $\mu$ M) treatment was applied during the growth phase (Figure S1a in the Supporting Information). TEM images also support the fact that treatment with CB[7] during the growth phase significantly reduces Ins fibril formation (Figure S1b). CB[7] also blocked Ins fibrillation under the acidic condition (pH 2.7, 0.1% formic acid v/v) although Ins fibrillation is promoted in these conditions (Figure 1d,e and Figure S1c,d).<sup>[13]</sup>

To better understand the inhibition of Ins fibrillation by CB[7], we investigated the interaction between CB[7] and Ins by using isothermal titration calorimetry (ITC) and native PAGE with wild-type Ins and its B-chain fragment mutants (Figure 1a and Figure S2). We confirmed that CB[7] binds solely to Phe-B1 of Ins ( $K_a = 4.4 \times 10^6 \text{ M}^{-1}$ ) in SPB solution (Figure S3b) as previously reported.<sup>[10]</sup> ITC measurements indicate that two CB[7] molecules can bind to Ins ( $K_{a1} = 3.8 \times 10^7 \text{ M}^{-1}$  and  $K_{a2} = 1.2 \times 10^4 \text{ M}^{-1}$ ) at pH 2.7 (Figure 1f and Table S1 in the Supporting Information). The experiments with single and multiple point mutants of Ins B-chain fragments indicate that Phe-B1 and Phe-B24 are the primary and the secondary binding sites for CB[7], respectively (Figure 1f and Figures S2–4). Because of the high binding affinity ( $K_{a1}$ ), almost complete binding of Phe-B1 with CB[7] occurred at all Ins:CB[7] ratios (Figure 1g). The Ins-2CB[7] complex was formed at low Ins:CB[7] ratios (1:5 and 1:10). The formation of Ins-1CB[7] and Ins-2CB[7] complexes was confirmed by matrix-assisted laser desorption ionization mass spectrometry (Figure S5). Circular dichroism (CD) measurements showed no significant structural change of Ins up to an Ins:CB[7] ratio of 1:1.5, where almost all Ins is present as the Ins-1CB[7] complex (Figure S6). However, a decrease in helical propensity was observed for the protein as the CB[7] concentration increased at pH 2.7. This finding indicates that the structural change in Ins is predominantly induced by the

secondary binding of CB[7] to Phe-B24. From a mechanistic point of view, the secondary binding of CB[7] to Phe-B24 is considered to prevent dimer formation. Ins dimerization, which is the initial step of the fibrillation,<sup>[14]</sup> is not well characterized, but residues B11–17 (LVEALYL)<sup>[14]</sup> and B24–26 (FFY)<sup>[15]</sup> have been considered to form the intermolecular interface that stabilizes the dimer (Figure 2). Phe-B1 is known to be involved in the oligomerization of Ins during the lag phase.<sup>[15]</sup> The suppression of fibril elongation at an Ins:CB[7] ratio of 1:0.5 implies that CB[7] can interact with oligomers. Thus, the binding of CB[7] to Phe-B1 seems to inhibit Ins oligomer formation. To obtain molecular insight into the effect of CB[7], molecular dynamics (MD) simulations were performed by using a structure for the partially folded Ins intermediate (PDB code: 1SF1; Figure S7) in water. In the initial state, two intermediate structures were positioned parallel with each other in the absence or presence of CB[7]. After 10 ns, the two intermediates without CB[7] underwent

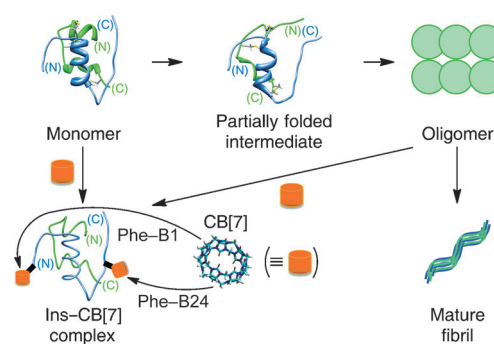


**Figure 2.** A schematic overview of Ins fibrillation and the inhibition mechanism of CB[7]. Monomer PDB ID: 2HIU, partially folded intermediate PDB ID: 1SF1.

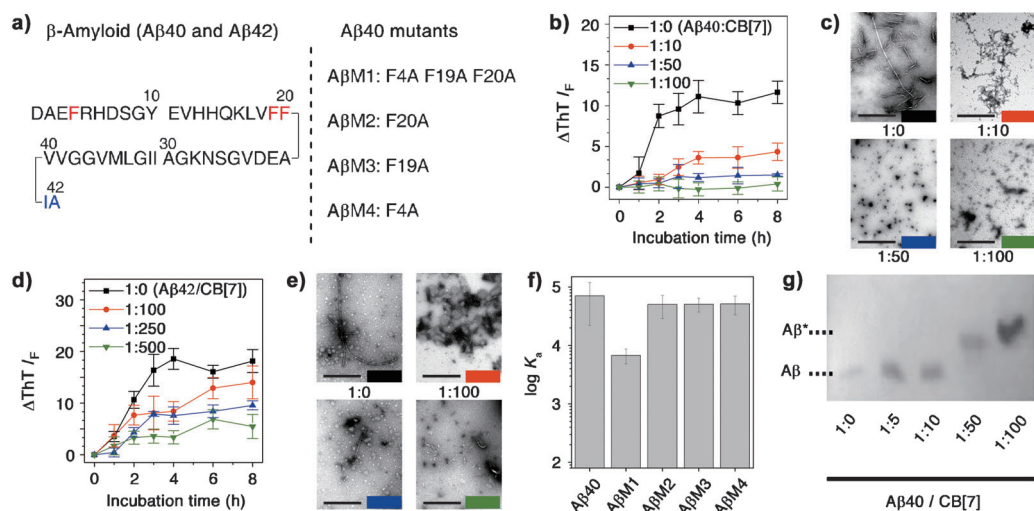


**Figure 3.** a) Sequences of the β-amyloid peptides Aβ40 and Aβ42, as well as Aβ40 mutants. The mutation sites are marked in red and the additional sequences of Aβ42 in blue. b) Fibrillation kinetics of Aβ40 with a series of Aβ40:CB[7] ratios in 20 mM SPB pH 7.4. c) TEM images of Aβ40 fibrils by Aβ40:CB[7] ratio after 8 h. d) Fibrillation kinetics of Aβ42 at a series of Aβ42:CB[7] ratios in 20 mM SPB pH 7.4. e) TEM images of Aβ42 fibrils by Aβ42:CB[7] ratio. f) Bar plots of the  $K_a$  values for Aβ40–CB[7] as measured by FDT (Figure S10). g) Native PAGE of the Aβ40–CB[7] complex (Aβ40\*). The concentrations of Aβ40 and Aβ42 were 5 μM. Scale bars: 500 nm.

dimerization in which the B11–17 and B24–26 residues formed an intermolecular contact. By contrast, in the case of the Ins–CB[7] complex, the formation of the intermolecular contact was prevented by the CB[7] molecule bound at Phe–B24. Overall, both the strong binding of CB[7] and the structural transformation contribute to the thermodynamic stabilization of Ins and the elevated activation energy for Ins fibrillation.

We also investigated the effect of CB[7] on the fibrillation of Aβ peptides (Figure 3a) in SPB solution (37 °C for Aβ40 and 25 °C for Aβ42). In the absence of CB[7], the ThT fluorescence signal of the Aβ40 sample (5 μM) increased spontaneously until it reached a plateau by approximately 4 h (Figure 3b). At a Aβ40/CB[7] ratio of 1:10, suppression of Aβ40 fibrillation was observed (Figure 3b,c). At Aβ40/CB[7] ratios of 1:50 and 1:100, Aβ40 fibrils were not observed. Adding CB[7] after incubation for 1 h caused a decrease in the final ThT fluorescence intensity and the fibrils were not found in the TEM images (Figure S8a,b). However, applying CB[7] to the Aβ40 sample after incubation for 3 h did not significantly affect fibrillation. Even for Aβ42, the fibrillation of which is extremely difficult to control owing to its fast fibrillation kinetics,<sup>[7]</sup> the ThT fluorescence intensity at the plateau decreased as the amount of CB[7] introduced into the solution increased, thus suggesting inhibition of fibrillation by CB[7] (Figure 3d). In accordance with the ThT result, the amount of fibrillation observed in the TEM images was reduced in the presence of CB[7] (Figure 3e). After the initiation of fibrillation, however, no inhibitory effect was observed on applying CB[7] (Figure S8c,d).

The host–guest interaction between CB[7] and Aβ40 was then examined by using the fluorescent dye titration (FDT) method (Figure 3f, Figures S9–11, and Table S2 in the Supporting Information).<sup>[16]</sup> The  $K_a$  value for the Aβ40–CB[7] complex was determined to be  $7.1 \times 10^4 \text{ M}^{-1}$  in SPB

solution (Figure 3f). Seven Aβ40 single and multiple point mutants (Figure 3a and Figure S11) were examined to determine the binding location of CB[7]. The results suggest that all three Phe residues (Phe–4, Phe–19, and Phe–20) are equally accessible to CB[7] and are thus responsible for the inhibition of fibrillation by complex formation with CB[7]. The Phe residues are considered to enhance hydrophobic clustering of the central region (His–13–Asp–23),<sup>[7]</sup> which is crucial for the formation of the partially folded intermediate for amyloid assembly

(Figure 4). Although Tyr shows weak binding to CB[7] (Figure 3f), the abundance of Phe–CB[7] is much higher than that of Tyr–CB[7], and Tyr is not directly involved in hydrophobic clustering.<sup>[7]</sup> The Phe–CB[7] interaction thus seems to be more crucial to the inhibitory effect of CB[7]. Native PAGE also indicates that the Aβ40–1CB[7] complex is observed as a distinct species with high concentrations of CB[7] (Figure 3g). CD spectroscopy reveals the structural shift of Aβ40 at 197 nm as the relative concentration of CB[7] increases (Figure S12). The structural change upon complex formation may prevent the additional binding of CB[7] to the peptide. Similarly, it is expected that the binding of CB[7] also disturbs the hydrophobic clustering of Aβ40. Aβ42 also forms a partially folded intermediate, but the formation rate is much higher than that for Aβ40.<sup>[7]</sup> CB[7] binds as tightly to Aβ42 as it does to Aβ40 and the same binding sites are expected owing to the identical sequence except for two additional residues

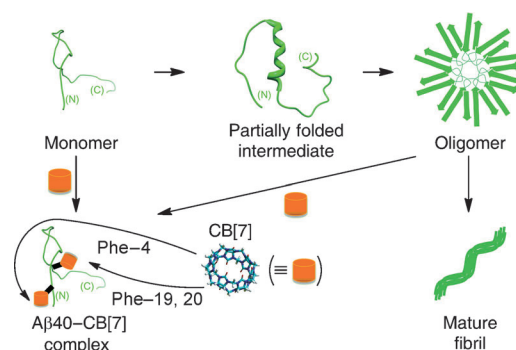


**Figure 4.** A schematic overview of Aβ fibrillation and the inhibition mechanism of CB[7]. Partially folded intermediate PDB ID: 2LFM. The oligomer structure is adopted from Ref. [21].



(Figure S13). Therefore, it is inferred that the inhibitory mechanism of CB[7] with A $\beta$ 42 is similar to that with A $\beta$ 40.

Among the amyloidogenic proteins investigated in the present study, the lag time decreases according to the trend Ins > A $\beta$ 40 > A $\beta$ 42 (Figure S14 and Table S3 in the Supporting Information).<sup>[7,17]</sup> The amount of CB[7] required for effective suppression of fibril formation increased with decreasing lag time of fibrillation. This result implies that the formation of protein–CB[7] complexes and protein oligomerization are competitive processes. CB[7] diffuses only 3–4 times faster than the Ins and A $\beta$  peptides<sup>[18]</sup> but the association rate for CB[7]–guest complex formation ( $10^8 \text{ M}^{-1} \text{ s}^{-1}$ )<sup>[19]</sup> is much higher than that of protein–protein interaction in the lag phase ( $10^{-2}$  and  $10^0 \text{ M}^{-1} \text{ s}^{-1}$  for Ins and A $\beta$ 40, respectively).<sup>[17]</sup> The inhibitory effect of CB[7] for both Ins and A $\beta$  is thus primarily driven by the faster rate of formation for the protein–CB[7] complex compared to protein–protein association. The association rate for the protein–protein interaction increases to  $10^3$ – $10^5 \text{ M}^{-1} \text{ s}^{-1}$  during the growth phase.<sup>[17]</sup> The addition of CB[7] may effectively prevent fibril formation up to a certain period in the growth phase, except with A $\beta$ 42, the fibrillation kinetics of which are much faster.<sup>[7]</sup>

The effective inhibition of fibril formation by CB[7] suggests potential utility of CB[7] for therapeutic applications in amyloid disease. A series of cell viability tests were performed to measure the effect of CB[7] on the cytotoxicity from Ins and A $\beta$  fibrils by using the 3-(4,5-dimethylthiazol-2-yl)-2,5-diphenyltetrazolium bromide (MTT) reduction assay (Figure 5). Ins fibrillation reduced the viability of NIH/3T3 cells to ca. 70% and both A $\beta$ 40 and A $\beta$ 42 fibrils reduced the viability of SH-SY5Y cells to ca. 75%. Applying CB[7] restored the cell viability of both NIH/3T3 and SH-SY5Y cells treated with protein fibrils to values comparable to the control group.

In summary, effective inhibition of amyloid fibrillation has been achieved by applying CB[7] at appropriate times during the fibrillation processes. It is also observed that CB[7] partially dissolves preformed fibrils, but further development will be needed to fully dissolve the fibrils on the basis of supramolecular host–guest chemistry. Unlike the  $\beta$ -cyclodextrins<sup>[6b]</sup> or molecular tweezers<sup>[6c]</sup> employed in earlier studies, CB[7] specifically captures Phe residues, which are directly involved in the hydrophobic clustering of amyloid processes,<sup>[20]</sup> thus causing the protein structures to be less amyloidogenic in the fibrillation process. The strong affinity of CB[7] for Phe ( $K_a$  of  $10^4$ – $10^7 \text{ M}^{-1}$ ) provides the present approach with an edge in terms of inhibiting amyloidosis compared to other small-molecule inhibitors. With the remarkable inhibitory activity of CB[7] toward protein fibrillation, the present study suggests a rational supramolecular strategy for blocking protein–protein interactions between amyloidogenic proteins by using a Phe-specific receptor.

Received: February 17, 2014

Revised: March 26, 2014

Published online: May 19, 2014

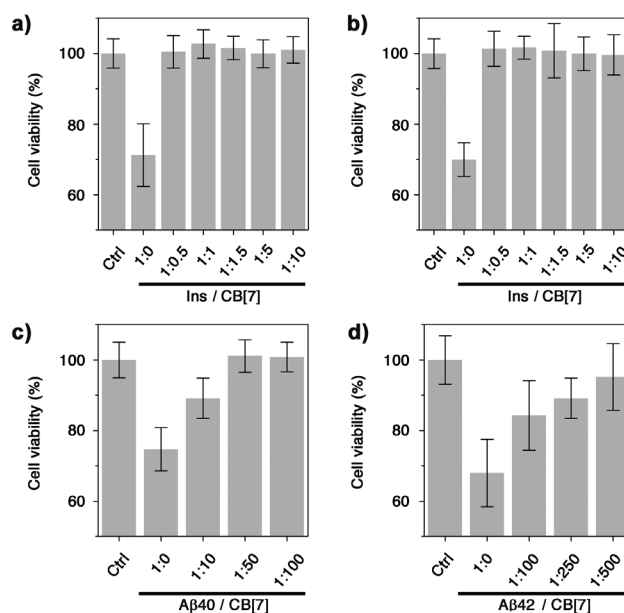


**Figure 5.** The inhibitory effect of CB[7] on the cytotoxicity of Ins, A $\beta$ 40, and A $\beta$ 42 fibrils. a) The addition of CB[7] decreased cytotoxicity of the Ins fibrils formed in 20 mM SPB pH 7.4 in NIH/3T3 cells. b) Cell viability was also rescued when CB[7] was applied at pH 2.7 [0.1% formic acid (v/v)]. c) Applying CB[7] to A $\beta$ 40 fibrils increased the survival rate of SH-SY5Y cells. d) Applying CB[7] also reduced the toxicity of A $\beta$ 42 fibrils. Additional data for the cytotoxicity and  $p$  values are available in Figures S15 and S17 and Tables S4–6.

**Keywords:** aggregation ·  $\beta$ -amyloid · cucurbit[7]uril · insulin · supramolecular chemistry

- [1] M. Goedert, M. G. Spillantini, *Science* **2006**, *314*, 777–781.
- [2] P. J. McLean, H. Kawamata, B. T. Hyman, *Neuroscience* **2001**, *104*, 901–912.
- [3] S. B. Prusiner, *Proc. Natl. Acad. Sci. USA* **1998**, *95*, 13363–13383.
- [4] A. E. Langkilde, B. Vestergaard, *FEBS Lett.* **2009**, *583*, 2600–2609.
- [5] T. Härd, C. Lendel, *J. Mol. Biol.* **2012**, *421*, 441–465.
- [6] a) S. S. Hinde, A. M. Mancino, J. J. Braymer, Y. Liu, S. Vivekanandan, A. Ramamoorthy, M. H. Lim, *J. Am. Chem. Soc.* **2009**, *131*, 16663–16665; b) A. Wahlström, R. Cukalevski, J. Danielsson, J. Jarvet, H. Onagi, J. Rebek, S. Linse, A. Gräslund, *Biochemistry* **2012**, *51*, 4280–4289; c) S. Sinha, D. H. J. Lopes, Z. M. Du, E. S. Pang, A. Shanmugam, A. Lomakin, P. Talbiersky, A. Tennstaedt, K. McDaniel, R. Bakshi, P. Y. Kuo, M. Ehrmann, G. B. Benedek, J. A. Loo, F. G. Klarner, T. Schrader, C. Y. Wang, G. Bitan, *J. Am. Chem. Soc.* **2011**, *133*, 16958–16969.
- [7] S. Vivekanandan, J. R. Brender, S. Y. Lee, A. Ramamoorthy, *Biochem. Biophys. Res. Commun.* **2011**, *411*, 312–316.
- [8] S.-Y. Seong, P. Matzinger, *Nat. Rev. Immunol.* **2004**, *4*, 469–478.
- [9] a) J. W. Lee, S. Samal, N. Selvapalam, H. J. Kim, K. Kim, *Acc. Chem. Res.* **2003**, *36*, 621–630; b) E. Masson, X. Ling, R. Joseph, L. Kyremeh-Mensah, X. Lu, *Rsc Adv.* **2012**, *2*, 1213–1247; c) J. Lagona, P. Mukhopadhyay, S. Chakrabarti, L. Isaacs, *Angew. Chem.* **2005**, *117*, 4922–4949; *Angew. Chem. Int. Ed.* **2005**, *44*, 4844–4870.
- [10] J. M. Chinai, A. B. Taylor, L. M. Ryno, N. D. Hargreaves, C. A. Morris, P. J. Hart, A. R. Urbach, *J. Am. Chem. Soc.* **2011**, *133*, 8810–8813.

- [11] F. E. Cohen, J. W. Kelly, *Nature* **2003**, *426*, 905–909.
- [12] M. D'Amico, M. G. Di Carlo, M. Groenning, V. Militello, V. Vetri, M. Leone, *J. Phys. Chem. Lett.* **2012**, *3*, 1596–1601.
- [13] J. L. Whittingham, D. J. Scott, K. Chance, A. Wilson, J. Finch, J. Brange, G. G. Dodson, *J. Mol. Biol.* **2002**, *318*, 479–490.
- [14] M. I. Ivanova, S. A. Sievers, M. R. Sawaya, J. S. Wall, D. Eisenberg, *Proc. Natl. Acad. Sci. USA* **2009**, *106*, 18990–18995.
- [15] L. Nielsen, S. Frokjaer, J. Brange, V. N. Uversky, A. L. Fink, *Biochemistry* **2001**, *40*, 8397–8409.
- [16] A. Hennig, H. Bakirci, W. M. Nau, *Nat. Methods* **2007**, *4*, 629–632.
- [17] C. C. Lee, A. Nayak, A. Sethuraman, G. Belfort, G. J. McRae, *Biophys. J.* **2007**, *92*, 3448–3458.
- [18] a) R. R. Walters, J. F. Graham, R. M. Moore, D. J. Anderson, *Anal. Biochem.* **1984**, *140*, 190–195; b) N. J. Wheate, P. G. A. Kumar, A. M. Torres, J. R. Aldrich-Wright, W. S. Price, *J. Phys. Chem. B* **2008**, *112*, 2311–2314; c) J. Waters, *Plos One* **2010**, *5*, e15709.
- [19] H. Tang, D. Fuentealba, Y. H. Ko, N. Selvapalam, K. Kim, C. Bohne, *J. Am. Chem. Soc.* **2011**, *133*, 20623–20633.
- [20] L. H. Tu, D. P. Raleigh, *Biochemistry* **2013**, *52*, 333–342.
- [21] S. Chimon, M. A. Shaibat, C. R. Jones, D. C. Calero, B. Aizezi, Y. Ishii, *Nat. Struct. Mol. Biol.* **2007**, *14*, 1157–1164.